Available online at www.sciencedirect.com
ScienceDirect
Appl. Comput. Harmon. Anal. 21 (2006) 262–267
Applied and Computational Harmonic Analysis
www.elsevier.com/locate/acha

Case Study

Wavelet inversion of the k-plane transform and its application ☆

Gangrong Qu

School of Sciences, Beijing Jiaotong University, Beijing, 100044, China

Received 14 December 2005; revised 24 January 2006; accepted 2 February 2006

Available online 9 March 2006

Communicated by Charles K. Chui

Abstract

We establish an inversion formula and a convolution–backprojection algorithm for the k-plane transform ($0 < k < n$) based on the wavelet theory. If $k = n - 1$, the proposed convolution–backprojection algorithm provides a novel method for the inversion of the Radon transform. We demonstrate that the proposed algorithm is easy to implement for global image reconstruction as well as local image reconstruction with the Lemarie–Mayer's wavelets.

Keywords: k-plane transform; Wavelet inversion formula; Convolution–backprojection algorithm

1. Introduction

The k-plane transform of a function f in R^n is its integral on k-dimensional planes of R^n. Assume that π is a k-dimensional plane of R^n. The k-plane transform of f is

$$R_\pi f(x'') = Rf(\pi, x'') = \int_\pi f(x' + x'')\,\mathrm{d}x', \tag{1}$$

where $x = x' + x''$ is the orthogonal direct sum decomposition of $x \in R^n$, $x' \in \pi$ and $x'' \in \pi^\perp$. The inversion of the k-plane transform is to find the function f given all $Rf(\pi, x'')$. All the k-dimensional subspaces in R^n forms the Grassmann manifold $G_{n,k}$. The k-plane Radon transform $Rf(\pi, x'')$ of a function $f \in L^2(R^n)$ is defined on a fibre bundle $T(G_{n,k})$ with base space $G_{n,k}$ and fibres isomorphic to R^{n-k}. When $k = n - 1$ or $k = 1$, $G_{n,k} = S^{n-1}$. Hence, for $k = n - 1$, Eq. (1) is the conventional Radon transform [9], $Rf(\omega, p) = \int_{x\cdot\omega=p} f(x)\,\mathrm{d}x = \int_{\omega^\perp} f(x' + p\omega)\,\mathrm{d}x'$.

☆ Supported by national natural science foundation of China (60372015) and the science foundation of Beijing Jiaotong University (2002SM54).
E-mail address: grqu@center.njtu.edu.cn.

1063-5203/$ – see front matter
doi:10.1016/j.acha.2006.02.004

Wavelet transform has been applied to find the inversions of the k-plane transforms in [1,6,10,12,13]. The recent developments of so-called ridgelet transforms have been promoted by D. Donoho, E.J. Candés and their collaborators [2,4]. Let ψ be a proper wavelet. The wavelet transform of $R_\pi f(x'')$ is

$$W_\psi R_\pi f(a,b) = \int_{\pi^\perp} R_\pi f(x'')\overline{\psi_{a,b}(x'')}\,\mathrm{d}x'' = |a|^{-\frac{n-k}{2}} \int_{R^n} f(x)\overline{\psi\left(\frac{|x-x'-b|}{a}\right)}\,\mathrm{d}x, \tag{2}$$

which is called the k-plane ridgelet transform of f. A Parseval-like relation for this transform in case $k = n-1$ has been established independently by Murata [7], Candés [2] and the author [10], from the perspective of neural networks, approximation theory and the inversion formula of Radon transform, respectively. Rashid-Farrokhi and et al. [11] proposed an algorithm to reconstruct the local image using local data and extra margin data in discrete wavelet case based on some wavelet bases with sufficiently many vanishing moments.

In the present paper, we developed a Parseval-like relation of the k-plane ridgelet transform equation (2). We derived a wavelet inverse formula for the k-plane transforms and established a convolution–backprojection algorithm for the k-plane transform. It is a generalization of the classical convolution–backprojection algorithm [5] in both forms and dimensional numbers and different from those in [12,13]. For R^2, the algorithm can be used to reconstruct local image as well as global image and is easier to implement utilizing less margin data than the algorithm in [11].

The paper is organized as follows. In Section 2, we derive the wavelet inversion formula and convolution–backprojection algorithm for the k-plane transform. In Section 3, we discuss implementation aspects and provide stimulation results for R^2.

2. The wavelet inversion and convolution–backprojection algorithm for the k-plane transform

In this section, we first prove an inversion formula for the k-plane ridgelet transform equation (2) in $L^2(R^n)$, and then a wavelet inversion formula and derive a convolution–backprojection algorithm for the k-plane transform. In this paper, for a fixed k, if $x = (x_1, \dots, x_n)$, we let $\bar{x} = (x_{k+1}, \dots, x_n)$ and $|\bar{x}| = \sqrt{x_{k+1}^2 + \dots + x_n^2}$. We assume that the wavelet function $\psi(s) \in L^2(R) \cap L^1(R)$ is an even function. Assume that $\Psi(\bar{x}) = \psi(|\bar{x}|)$. The Fourier transform of $\Psi(|\bar{x}|)$ with respect to $\bar{x}$ is $\hat{\Psi}(\bar{\xi}) = \int_{R^{n-k}} \psi(|\bar{x}|)e^{-2\pi i \bar{x}\cdot\bar{\xi}}\,\mathrm{d}\bar{x}$. It is easy to show that $\hat{\psi}(\bar{\xi})$ is radially symmetric, i.e., $\hat{\Psi}(\bar{\xi}) = \hat{\Psi}_0(|\bar{\xi}|)$ for some function $\hat{\Psi}_0$. For a fixed k, the admissible condition of the wavelet $\psi(|\bar{x}|)$ is $C_{\psi,k} = \int_{-\infty}^{\infty} \frac{|\hat{\Psi}_0(a)|^2}{|a|^{k+1}}\,\mathrm{d}a < \infty$. Let $\psi_{a,b}(x) = |a|^{-\frac{n-k}{2}}\psi\left(\frac{|x-b|}{a}\right)$.

Let $\{e_1, \dots, e_k\}$ be an orthonormal system in R^n. The matrix W formed by $W = (e_1, \dots, e_n)$ is an orthogonal matrix. Let π_0 be the subspace of R^n spanned by $\{e_1, \dots, e_k\}$. $\{e_1, \dots, e_k\}$ is an orthonormal basis of π_0. Because $x' \in \pi$ and $x'' \in \pi^\perp$, we let

$$x = x' + x'' = \pi_0(t_1, \dots, t_k)^T + (e_{k+1}, \dots, e_n)(t_{k+1}, \dots, t_n)^T,$$

where $t_i = e_i^T x$, $i = 1, \dots, n$. Hence, $x' = \pi_0\pi_0^T x$ and Eq. (2), the wavelet transform of $R_\pi f(x'')$, can be written as $Tf(\pi_0, a, b) = |a|^{-\frac{n-k}{2}} \int_{R^n} f(x)\overline{\psi\left(\frac{|x-\pi_0\pi_0^T x-b|}{a}\right)}\,\mathrm{d}x$.

Lemma. [14] *Let $f(x) \in L^1(R^n)$. Then $\int_{R^n} f(x)\,\mathrm{d}x = \int_{G_{n,k}} \int_{\pi^\perp} f(x)|x|^k\,\mathrm{d}x\,\mathrm{d}\mu$.*

Theorem 1. *Let $f \in L^2(R^n)$ have compact support and g belong to the Schwartz space $\mathcal{S}(R^n)$. Then*

$$\int_{G_{n,k}} \mathrm{d}\mu \int_{-\infty}^{\infty} \mathrm{d}a \int_{\pi^\perp} Tf(\pi_0, a, b)\overline{Tg(\pi_0, a, b)}\frac{\mathrm{d}b}{|a|^{n+1}} = C_\psi\langle f, g\rangle, \tag{3}$$

and

$$f(x) = C_\psi^{-1} \int_{G_{n,k}} \mathrm{d}\mu \int_{-\infty}^{\infty} \frac{\mathrm{d}a}{|a|^{2n-k+1}} \int_{\pi^\perp}\int_{\pi^\perp} R_\pi f(x'')\overline{\psi\left(\frac{|x''-b|}{a}\right)}\,\mathrm{d}x''\,\psi\left(\frac{|x-\pi_0\pi_0^T x-b|}{a}\right)\mathrm{d}b \tag{4}$$

weakly in L^2. At any continuous point of f, the equality (4) *holds in pointwise.*

Proof. In Eq. (3), let $x = Wz$ and $b = Wb'$. Because $b \in \pi^{\perp}$, we let $b' = (0, \ldots, 0, b'_{k+1}, \ldots, b'_n)$ and so

$$x - \pi_0 \pi_0^T x - b = (e_{k+1}, \ldots, e_n)(\bar{z} - \overline{b'}). \tag{5}$$

Using the Parseval equality with respect to variable $\bar{z}$ in the following, we then obtain

$$Tf(\pi_0, a, b) = |a|^{-\frac{n-k}{2}} \int_{R^n} f(Wz) \overline{\psi\left(\frac{|\bar{z} - \overline{b'}|}{a}\right)} \, dz = |a|^{\frac{n-k}{2}} \int_{R^{n-k}} \hat{f}(W\xi') \overline{\hat{\Psi}_0(a|\bar{\xi}|)} e^{-2\pi i \overline{b'} \cdot \bar{\xi}} \, d\bar{\xi}, \tag{6}$$

where $\xi' = (0, \ldots, 0, \xi_{k+1}, \ldots, \xi_n)^T$ and $\bar{z} \cdot \bar{\xi} = z \cdot \xi'$. In the left-hand side of Eq. (3), we interchanged the integral orders with respect to z and b by Fubini's theorem and get

$$\int_{\pi^{\perp}} e^{-2\pi i b \cdot \xi} \psi\left(\frac{|\bar{y} - \overline{b'}|}{a}\right) db = \int_{R^{n-k}} e^{-2\pi i \bar{b} \cdot \bar{\xi}} \psi\left(\frac{|\bar{y} - \overline{b'}|}{a}\right) d\overline{b'} = |a|^{(n-k)} e^{2\pi i y \cdot \xi'} \hat{\Psi}_0(a|\xi|) \tag{7}$$

and

$$\int_{-\infty}^{\infty} \frac{|\hat{\psi}_0(a|\bar{\xi}|)|^2}{|a|^{k+1}} \, da = |\bar{\xi}|^k \int_{-\infty}^{\infty} \frac{|\hat{\Psi}_0(a)|^2}{|a|^{k+1}} \, da = C_{\psi,k} |\bar{\xi}|^k.$$

By Lemma, we find that the left-hand side of Eq. (7) is equal to

$$C_{\psi,k} \int_{G_{n,k}} \int_{R^{n-k}} \hat{f}(W\xi') \overline{\hat{g}(W\xi')} |\bar{\xi}|^k \, d\xi' \, d\mu = C_{\psi,k} \int_{R^n} f(x) \overline{g(x)} \, d\xi. \tag{8}$$

Therefore Eq. (3) holds. Because the Schwartz space $\mathcal{S}(R^n)$ is dense in $L^2(R^n)$, it follows that Theorem 1 holds by letting α tend to zero for a Gaussian function $g(x) = g_\alpha(x)$, where α is the standard variance of the Gaussian function. □

We also have the following convergent result in $L^2(R^n)$.

Theorem 2. *If function $f(x) \in L^2(R^n)$ has compact support, then*

$$\lim_{\substack{A_1 \to 0 \\ A_2, B \to \infty}} \left\| f(x) - C_{\psi,k}^{-1} \int_{G_{n,k}} d\mu \int_{A_1 < |a| < A_2} \frac{da}{|a|^{k+1}} \times \int_{\pi^{\perp} \cap \{|b| < B\}} \int_{\pi^{\perp}} R_\pi f(x'') \overline{\psi\left(\frac{|x'' - b|}{a}\right)} dx'' \psi\left(\frac{|x - \pi_0 \pi_0^T - b|}{a}\right) db \right\|_{L^2} = 0.$$

The proof of Theorem 2 is the same as the proof of Property 1.4.1 of [3]. It is skipped due to the space limit.

By Theorems 1 and 2, we obtain the following two theorems.

Theorem 3. *Assume $f \in L^2(R^n)$ have compact support. Then*

$$\lim_{A \to \infty} \left\| f(x) - \int_{G_{n,k}} d\mu \int_{\pi^{\perp}} R_\pi f(x'') q_A(x - \pi_0 \pi_0^T x - x'') \, dx'' \right\|_{L^2} = 0, \tag{9}$$

at any continuous point of f, and $\lim_{A \to \infty} |f(x) - \int_{G_{n,k}} d\mu \int_{\pi^{\perp}} R_\pi f(x'') q_A(x - \pi_0 \pi_0^T x - x'') \, dx''| = 0$, where $F_A(a) = 2C_{\psi,k}^{-1} \int_{\frac{2a}{A}}^{\infty} \frac{|\hat{\Psi}_0(s)|^2}{s^{k+1}} \, ds$, $q_A(t) = 2|S^{n-k-2}| \int_0^{\infty} F_A(a) a^{n-1} h(2\pi a t) \, da$.

Theorem 4. *Assume that the function* $f \in L^2(R^n)$ *has compact support. Then*

$$\lim_{A\to\infty}\left\| f(x) - \int_{|\omega|=1} \mathrm{d}\omega \int_{-\infty}^{\infty} Rf(t,\omega) q_A(x\cdot\omega - t)\,\mathrm{d}t \right\|_{L^2} = 0, \tag{10}$$

at any continuous point of f, *and* $\lim_{A\to\infty} |f(x) - \int_{|\omega|=1} \mathrm{d}\omega \int_{-\infty}^{\infty} Rf(t,\omega) q_A(x\cdot\omega - t)\,\mathrm{d}t| = 0$, *where* $F_A(a) = 2C^{-1}_{\psi,n-1} \int_{2a/A}^{\infty} \frac{|\hat\psi(\xi)|^2}{\xi^n}\,\mathrm{d}\xi$ *and* $q_A(t) = 2\int_0^\infty F_A(a) a^{n-1}\cos(2\pi a t)\,\mathrm{d}a$.

3. Implementation and simulation results in R^2

Wavelet windows can be selected in various ways. Here we choose the wavelets such that $\operatorname{supp}[\hat\psi(\xi)] \in [-1,1]$ and $\hat\psi(\xi) \in C^\infty$. Hence $F_A(a) \in C^\infty$. $F_A(a)$ is different from the window functions of the classical convolution–backprojection that are discontinuous at the endpoints of the windows [5]. It turns out in the following that the smoothness of $\hat\psi(\xi)$ is critical for local image reconstruction. Therefore we choose one of Lemarie–Mayer's wavelets [8]. Let

$$\alpha(t) = \begin{cases} e^{\frac{1}{1-|t|^2}}, & |t|<1 \\ 0, & |t|\geqslant 1 \end{cases}, \quad \alpha_1(t) = C_1\alpha\left(\frac{t}{\frac{\pi}{3}}\right), \quad \alpha_2(t) = C_2\alpha\left(\frac{t}{\frac{2\pi}{3}}\right),$$

where C_i is the constants such that $\int_{-\infty}^{\infty} \alpha_i(t)\,\mathrm{d}t = \frac{\pi}{2}$, $\theta_i(t) = \int_{-\infty}^{t} \alpha_i(\tau)\,\mathrm{d}\tau$ and $s_i(t) = \sin\theta_i(t)$, $i = 1,2$. Let $b_1(t) = s_1(t-\pi)s_2(-t+2\pi)$ and $\hat\psi_1(\xi) = b_1(\xi)e^{i\frac{\xi}{2}}$. $\hat\psi_1 \in C^\infty$. Let $\hat\psi(\xi) = \hat\psi_1(\frac{8\pi}{3}\xi)$. Then $\operatorname{supp}\hat\psi \subset [-1,1]$.

The left- and right-hand sides of Fig. 1 are 512×512 pixel image of the original Shepp–Logan head phantom and reconstructed image respectively by our algorithms using global data.

Now we discuss the problem of local reconstruction. Suppose $f(x) \in L^\infty(R^2)$ has a compact support. Then $Rf(\omega,s) \in L^\infty(Z)$. Let $B(x_0,t) = \{x \mid |x-x_0| \leqslant t\}$. We are to reconstruct the image on $B(x_0,R)$ using the projection data $Rf(t,\theta)$ through $B(x_0,R+\tau)$. Using integration by parts, we get

$$q(s) = -\frac{2}{(2\pi s)^2} + \frac{C(s)}{(2\pi s)^m}, \tag{11}$$

$$q_A(s) = A^2 q(As) = -\frac{2}{(2\pi s)^2} + \frac{C(As)}{A^{m-2}(2\pi s)^m} \quad (s\to\infty), \tag{12}$$

for $s \neq 0$ where m is a positive integer, $|C(s)| \leqslant C_m = \int_0^{1/2} |mF^{(m-1)}(a) + aF^{(m)}(a)|\,\mathrm{d}a$. Let

$$f_A(x) = \int_{|\omega|=1} \mathrm{d}\omega \int_{-\infty}^{+\infty} Rf(t,\theta) q(x\cdot\omega - t)\,\mathrm{d}t, \tag{13}$$

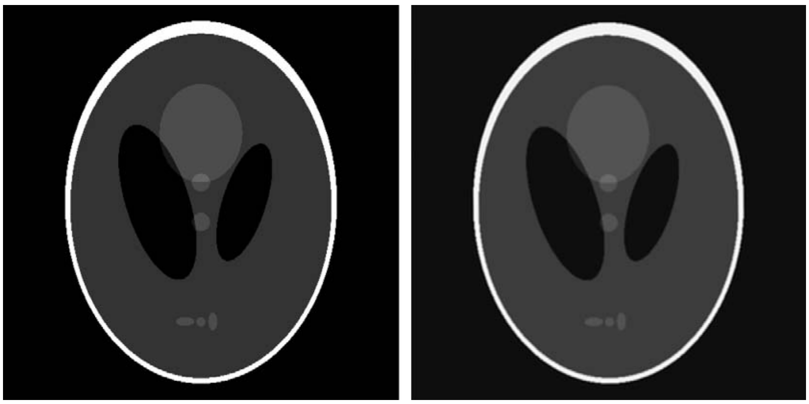

Fig. 1. (a) Original image, (b) reconstructed image.

$$f_R(x) = \int_{|\omega|=1} \mathrm{d}\omega \int_{-R-\tau+x_0\cdot\omega}^{R+\tau+x_0\cdot\omega} Rf(t,\theta)q(x\cdot\omega - t)\,\mathrm{d}t. \tag{14}$$

We have $f_E(x) = f_A(x) - f_R(x) = \int_{|\omega|=1} \mathrm{d}\omega \int_{|t-x_0\cdot\omega|\geqslant R+\tau} Rf(t,\theta)q(x\cdot\omega - t)\,\mathrm{d}t$. By the convolution–backprojection algorithm, it follows that $f_A(x)$ is the global reconstructed image, $f_R(x)$, where $x \in B(x_0, R)$, is the reconstructed local image, and $f_E(x)$ is the truncated error. Let $f_E(x) - f_E(x_0) = R_1 + R_2$,

$$R_1 = -\frac{1}{2\pi^2} \int_{|\omega|=1} \mathrm{d}\omega \int_{|t|>R+\tau} Rf(t + x_0\cdot x, \omega)\left(\frac{1}{(t-(x-x_0)\cdot\omega)^2} - \frac{1}{t^2}\right)\mathrm{d}t,$$

$$R_2 = -\frac{2}{A^{m-2}(2\pi)^m} \int_{|\omega|=1} \mathrm{d}\omega \int_{|t|>R+\tau} Rf(t + x_0\cdot\omega, \omega)\left(\frac{C(A(t-(x-x_0)\cdot\omega))}{(t-(x-x_0)\cdot\omega)^m} + \frac{C(At)}{t^m}\right)\mathrm{d}t.$$

By Shwartz's inequality, $|R_1| \leqslant C_1(R, R+\tau)\|Rf\|_{L^2(Z)}$, where

$$C_1(R, R+\tau) = \frac{1}{2\pi^2}\left(\int_0^{2\pi} \int_{|t|\geqslant R+\tau} \left(\frac{1}{(t-(x-x_0)\cdot x)^2} - \frac{1}{t^2}\right)^2 \mathrm{d}t\,\mathrm{d}\theta\right)^{1/2}$$

is a small number [9]. If $x \in B(x_0, R)$ and the margin data has k pixels, then

$$|R_2| \leqslant \frac{8C_m\pi\|Rf\|_{L^\infty(Z)}}{(m-2)A^{m-1}(2\pi)^m}\frac{1}{\tau^{m-1}} \leqslant \inf_{m>2}\frac{4C_m\|Rf\|_{L^\infty(Z)}}{(m-1)k^{m-1}(2\pi)^{m-1}d},$$

where d is the length of radial sampling interval of the projection data, $A = 1/d$, R_2 depends on C_m and hence depends on the chosen wavelet. In order to eliminate the unknown constant bias, we extrapolate the projections continuously by constant extension on the missing projections [11]

$$(Rf)_{\mathrm{local}}(t,\omega) = \begin{cases} (Rf)(t,\omega), & \text{if } |x_0|\omega\cdot\omega_0 - (R+\tau) \leqslant t \leqslant |x_0|\omega\cdot\omega_0 + R + \tau, \\ (Rf)(R+\tau+x_0\cdot\omega, \omega), & \text{if } t > |x_0|\omega\cdot\omega_0 + R + \tau, \\ (Rf)(-R-\tau+x_0\cdot\omega, \omega), & \text{if } t < |x_0|\omega\cdot\omega_0 - (R+\tau). \end{cases}$$

We use $(Rf)_{\mathrm{local}}(t + x_0\cdot\omega, \omega)$ as projection data to reconstruct the local image. Now for $x \in B(x_0, R)$, the local reconstructed image is given as $f_{\mathrm{local}}(x) = \int_{|\omega|=1} \mathrm{d}\omega \int_{-\infty}^{+\infty} Rf_{\mathrm{local}}(t,\theta)q(x\cdot\omega - t)\,\mathrm{d}t$.

Fig. 2. (a) Original image, (b) reconstructed image.

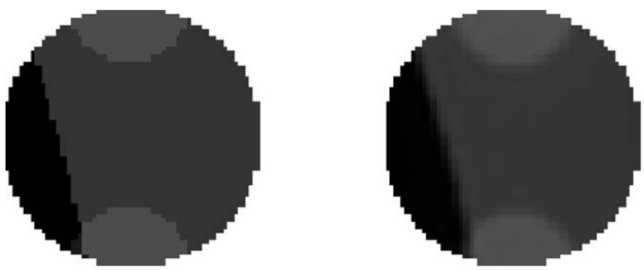

Fig. 3. (a) Original image, (b) reconstructed image.

The right- and left-hand sides of Figs. 2 and 3 are the radius 50, 25 pixels local original image of Shepp–Logan 512×512 phantom and the reconstructed local images using local data with 4 pixels extra margin, respectively.

Acknowledgments

The author thanks the anonymous referees for valuable remarks and constructive suggestions.

References

[1] C.A. Berenstein, D.F. Walnut, Local inversion of the Radon transform in even dimensions using wavelets, in: S. Gindikin, P. Michor (Eds.), 75 Years of Radon Transform, International Press, Cambridge, MA, 1994, pp. 45–69.
[2] E.J. Candés, Harmonic analysis of neural networks, Appl. Harmon. Anal. 6 (2) (1999) 197–218.
[3] I. Daubechies, Ten Lectures on Wavelets, CBMS-NSF Series in Appl. Math., SIAM, 1991.
[4] D. Donoho, Ridge functions and orthonormal ridgelets, J. Approx. Theory 111 (2001) 143–179.
[5] G.T. Herman, Image Reconstruction from Projection, Academic Press, New York, 1980.
[6] M. Holschneider, Inverse Radon transform through inverse wavelet transform, Inverse Problems 7 (1991) 853–861.
[7] N. Murata, An integral representation with ridge functions and bounds of three-layered networks, Neural Networks 9 (6) (1996) 947–956.
[8] E. Hernadez, G. Weiss, A First Course on Wavelets, CRC Press, New York.
[9] F. Natterer, The Mathematics of Computerized Tomography, Wiley, New York, 1986.
[10] G. Qu, Inverse Radon transform with one-dimensional wavelet transform, Acta Math. Appl. Sin. 16 (1) (2000) 70–77.
[11] F. Rashid-Farrokhi, K.J.R. Liu, C. Berenstein, D. Walnut, Wavelet-based multiresolution local tomography, IEEE Trans. Image Process. 6 (10) (1997) 159–166.
[12] B. Rubin, Inversion of Radon transforms using wavelet transforms generated by wavelet measures, Math. Scand. 85 (1999) 285–300.
[13] B. Rubin, Convolution–backprojection method for the k-plane transform, and Calderón's identity for ridgelet transforms, Appl. Comput. Harmon. Anal. 16 (2004) 231–242.
[14] D.C. Solmon, The X-ray transform, J. Math. Anal. Appl. 56 (1976) 61–83.